J Supercond Nov Magn (2016) 29:1387–1397
DOI 10.1007/s10948-016-3434-1

ORIGINAL PAPER

# Theoretical Investigation of Half-metallic Ferromagnetism in $Mg_{0.75}Ti_{0.25}Y$ (Y = S, Se, Te) Alloys by Using DFT-mBJ Studies

**Q. Mahmood[1] · S. M. Alay-e-Abbas[2,3] · M. Yaseen[4] · Asif Mahmood[5] · M. Rashid[6] · N. A. Noor[7]**

Received: 20 January 2016 / Accepted: 22 January 2016 / Published online: 5 February 2016


**Abstract** The full-potential linear-augmented-plane-waves plus local-orbitals (FP-LAPW+lo) method has been employed to explore the mechanical and half-metallic ferromagnetic properties of Ti-doped ordered zinc-blende MgS, MgSe, and MgTe semiconductors. Ductile and partial ionic natures of subjected compounds are investigated in terms of Poisson's and Pough ratios, while the anisotropy value is evaluated to affirm the preferred orientation properties of these materials. Two different formalism of exchange and correlation (XC) effects have been applied in the form of generalized gradient approximation (GGA) and orbital independent modified Becke-Johnson potential combined with local density approximation (mBJLDA). Enthalpy of formation and energetic comparison has been used to establish the stability of ferromagnetic (FM). Premeditated electronic properties divulge that the Ti-doping induces ferromagnetism in MgS, MgSe, and MgTe which appear to show half-metallic (HM) gap at Fermi level ($E_F$). In addition, the calculated electronic properties are analyzed in terms of the $s-d$ and $p-d$ exchange constants ($N_0\alpha$ and $N_0\beta$) that are found to be comparable with typical magneto optical experiment.

**Keywords** First-principle calculations · Half-metallic ferromagnetic · Electronic structure · Magnetic properties

✉ N. A. Noor
naveedcssp@gmail.com

M. Yaseen
myaseen_taha@yahoo.com

[1] Department of Physics, University of the Punjab, Quaid-e-Azam Campus, 54590 Lahore, Pakistan

[2] Department of Physics, Government College University Faisalabad, Allama Iqbal Road, Faisalabad 38000, Pakistan

[3] Department of Physics, University of Sargodha, Sargodha 40100, Pakistan

[4] Department of Physics, University of Agriculture, Faisalabad, 38040, Pakistan

[5] College of Engineering, Chemical Engineering Department, King Saud University, Riyadh, Saudi Arabia

[6] Department of Physics, COMSATS Institute of Information Technology, 44000 Islamabad, Pakistan

[7] Centre for High Energy Physics, University of the Punjab, Quaid-e-Azam Campus, 54590 Lahore, Pakistan

## 1 Introduction

Owing to their potential for computing complex structural and electronic properties of solids with great accuracy has made first-principle calculations an important tool of materials research [1–4]. This advancement in simulation techniques has brought many breakthroughs in condensed matter physics. For instance, we can analyze those (non-magnetic and magnetic) properties of materials [5–8] which were very hard to be studied through experiments. Also, such properties which needed very intense imaginative insight are now possible to be explained through virtual reality with the help of computational methods.

Dilute magnetic semiconductors (DMS) [9] are renowned magnetic materials which can be made by doping traditional semiconductors with transition metal impurities. In order to use DMS based on II–VI and III–V semiconductor compounds practically, it is necessary that these

compounds possess a unique combination of structural, electronic, and magnetic properties. In DMS solid solution, the cations are usually replaced by magnetic transition metal and/or rare-earth anions. Hence, the nature and concentration of the dopant firmly decides the structural, electronic, and magnetic properties of DMS. It is worth pointing out here that doping does not enforce the host to drop off its semiconducting properties rather than it furnishes magnetic effects in the host [10].

Another important feature of doped semiconductors is that the dopant composition can control energy band gaps and other important physical properties [11]. Also, doped semiconductors have the ability to regulate charge as well as electronic spin current which makes them among the promising candidates for spintronic devices [12]. The prime purpose behind the wide spread research on magnetic materials is to manufacture the feasible devices like ultra-fast optical switches, spin LEDs, spin valves, and magnetic sensor in spintronic industry [13]. Many researchers [14–17] have analyzed (theoretically and experimentally) the response of adding the magnetic transition elements (Ti, Mn, Fe, Co, Ni, and Cr) and rare-earth elements (like Sm, Er, Dy, Gd) into the conventional semiconductors (either II–VI or III–V) compounds.

The II–VI systems, magnesium chalcogenides, MgX (X = S, Se, Te), in fourfold coordinate ZB structure that can be crystallized at low pressure. Their small ionic radii and strong covalent binding nature are the prime features which make them distinct from all other alkaline-earth metal chalcogenides. For these compounds, the Philips ionicity, band gap, and bulk modulus values increases while going from MgTe to MgS [18, 19]. Larger values of bulk modulus make them more stable materials. Furthermore, MgS and MgTe have lattice constants closer to those of gallium arsenide and zinc selenide. Keeping in view all these appealing characteristics, magnesium chalcogenides are promising materials for optoelectronic devices [20, 21]. In the present study, we have investigated structural, electronic, and magnetic properties of Ti doped on zinc blende MgY (Y = S, Se, and Te) semiconductor. The 3d transition element Ti is adopted with the purpose to introduce magnetism in the paramagnetic MrY compounds for which no theoretical work has been carried out yet, to the best of our knowledge.

## 2 Method of Calculations

To evaluate the ground state properties of Ti-doped Mg-chalcogenides, full-potential linearized augmented plane (FP-LAPW+lo) method is used which has its basis on density functional theory (DFT) and incorporated into wien2k code to solve the many electron system [22]. From this method, eigenvalue and eigenfunction of Kohn-Sham equations are calculated systematically [23]. In order to solve the electron core interaction problem (exchange co-relation potential), generalized gradient approximation (GGA) is used to evaluate the ground state parameters of material and its mechanical response [24]. The electronic and magnetic properties are computed by the implementation both modified Becke-Johnson exchange potential [25] and local density approximation combinedly called as mBJLDA. The joint effect of semi-local exchange potential and local spin density gives the improved energy band gap of spin polarized semiconductors and transition metal (TM)-doped materials [26–29].

In this work, the core and valence states of the Mg, Ti, and Y = S, Se, Te are behaved as self-consistently in

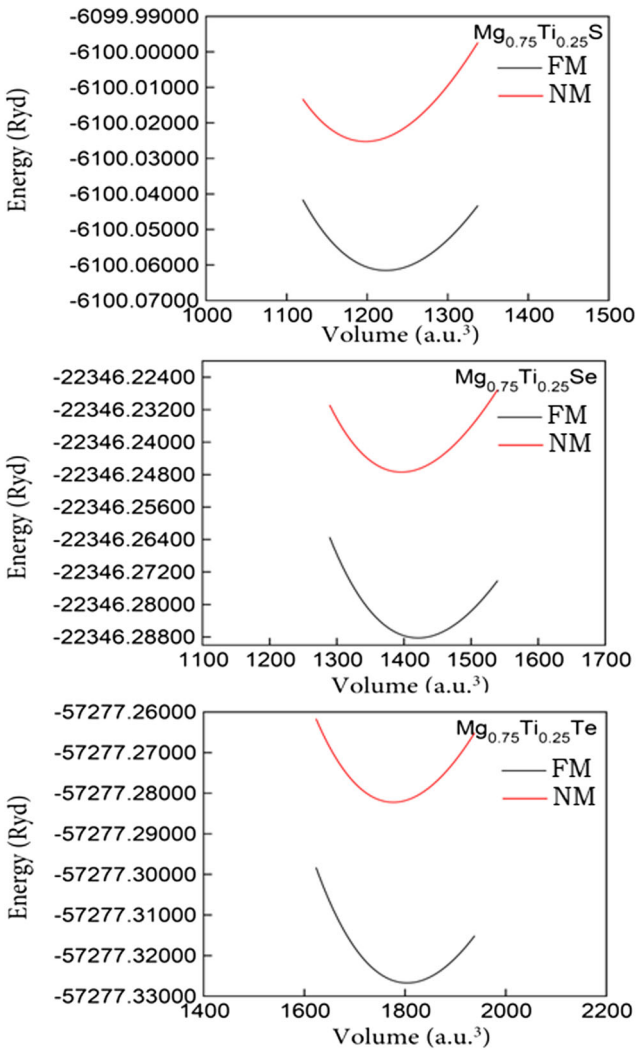


**Fig. 1** Total energy verses unit cell volume for $Mg_{0.75}Ti_{0.25}Y$ (Y = S, Se, Te) alloys in non-magnetic (NM) and ferromagnetic (FM) phase

**Table 1** Equilibrium lattice constant $a$ (Å), bulk modulus $B$ (GPa), total energy difference $\Delta E$ (eV), crystal field energy ($\Delta E_{crystal}$), band gap values $E_g$ (eV) and enthalpies of formation $\Delta H_f$ (eV) calculated for MgTiY (Y = S, Se, Te)

| Compound | $a$ (Å) | $B$ (GPa) | $E_g$ (eV) | ($E_{HM}$) | $\Delta E$ (eV) | $\Delta H_f$ (eV) |
|---|---|---|---|---|---|---|
| MgS | 5.62 | 68.01 | 4.75 | | | −3.61 |
| Exp. | 5.619[a] | | 4.50[d] | | | |
| Others | 5.61[c] | 61.20[c] | 3.37[c] | | | |
| $Mg_{0.75}Ti_{0.25}S$ | 5.65 | 60.09 | 4.88 | 1.50 | 0.4935 | −2.63 |
| MgSe | 5.88 | 57.91 | 4.08 | | | −1.12 |
| Exp. | 5.89[a] | | 3.60[e] | | | |
| Others | 5.88[c] | 50.50[c] | 2.82[c] | | | |
| $Mg_{0.75}Ti_{0.25}Se$ | 5.97 | 49.97 | 4.29 | 1.55 | 0.5554 | −1.48 |
| MgTe | 6.36 | 43.72 | 3.41 | | | −1.35 |
| Exp. | 6.36[b] | | 3.47[f] | | | |
| Others | 6.38[c] | 38.70[c] | 2.61[c] | | | |
| $Mg_{0.75}Ti_{0.25}Te$ | 6.47 | 40.31 | 3.45 | 1.57 | 0.6051 | −1.17 |

[a]Ref [55]
[b]Ref [56]
[c]Ref [57]
[d]Ref [58]
[e]Ref [59]
[f]Ref [60]

relativistically relaxed, spherical approximation and semi-relativistic approximation (without spin-orbit coupling), respectively. The charge density, wave function, and potential expanded within the non-overlapping spheres surrounded by the atomic sties and the residual (interstitial) space of the unit cell by the plane-wave basis set. For the wave expansion in the atomic sphere, maximum quantum number $l_{max}$ is chosen as 10 and the Fourier-expanded charge density $G_{max}$ up to 20 $(Ry)^{1/2}$. $R_{MT} \times k_{max}$ known as convergence parameter, that controls the dimension of the basis set, is fixed to 8. The average radius of the muffin tin spheres is represented by $R_{MT}$, and for reciprocal lattice, the maximum modulus is represented by $k_{max}$. We have used the muffin tin radius values for the Ti, Mg, S, Se, and Te as 1.96, 1.68, 2, and 1.73 atomic units (a.u.), respectively. The $10 \times 10 \times 10$ Monkhorst–Pack mesh along with sufficient $k$-vectors in the irreducible Brillion zone is used to model the reciprocal space. In each evaluation, we have converged the total energy of crystal up to $10^{-5}$ Ry by recurrence process.

**Table 2** Calculated elastic constants $C_{ij}$ (GPa), Kleinman parameters ($\zeta$), shear modulus $G$ (GPa), Young's modulus $E$ (GPa), Poisson's ratio, anisotropy factor ($A$) and B/G ratio at equilibrium for binary compounds and their alloys $Mg_{1-x}Ti_xY$ (Y = S, Se and Te) at $x = 0$, 0.25

| Compound | C11 | C12 | C44 | $B_0$ | $\zeta$ | $G$ | $E$ | $V$ | $A$ | B/G |
|---|---|---|---|---|---|---|---|---|---|---|
| MgS (cal.) | 87.1 | 58.5 | 65.4 | 68.0 | 0.76 | 35.94 | 91.59 | 0.275 | 4.59 | 1.89 |
| Exp[a]. | – | – | – | | – | – | – | – | – | – |
| Other cal. | 72.2[a] | 55.7[a] | 58.4[a] | | – | – | – | – | – | – |
| $Mg_{0.75}Ti_{0.25}S$ | 70.1 | 55.1 | 50.5 | 60.1 | 0.85 | 24.35 | 64.35 | 0.322 | 6.72 | 2.47 |
| MgSe (cal.) | 63.8 | 54.9 | 53.5 | 57.8 | 0.802 | 21.91 | 58.36 | 0.332 | 11.9 | 2.64 |
| Exp. | | | | | | | | | | |
| Other cal. | 63.2[a] | 43.8[a] | 44.7[a] | | | | | | | |
| $Mg_{0.75}Ti_{0.25}Se$ | 61.8 | 44.2 | 41.7 | 50.1 | 0.796 | 21.82 | 57.20 | 0.309 | 4.39 | 2.29 |
| MgTe (cal.) | 49.8 | 40.6 | 54.5 | 43.6 | 0.872 | 22.38 | 59.07 | 0.281 | 11.8 | 1.95 |
| Exp. | | | | | | | | | | |
| Other cal. | 61.2[a] | 28.2[a] | 48.2[a] | | | | | | | |
| $Mg_{0.75}Ti_{0.25}Te$ | 51.9 | 34.4 | 39.1 | 40.23 | 0.758 | 21.68 | 55.16 | 0.274 | 4.21 | 1.85 |

[a]Ref. [57]

## 3 Result and Discussion

### 3.1 Structural Properties

On computational grounds, structural optimization is of enormous concern to obtain the ground state properties of a material. In this process, we have performed the structural optimization for ZB $Mg_{0.75}Ti_{0.25}Y$ (Y = S, Se, Te) compounds with WC-GGA through total energy minimization as a function of unit cell volume in order to obtain optimized lattice parameters ($a_0$) and bulk moduli ($B_0$). The total energy versus volume curves at $x = 0.25$ are displayed in Fig. 1; however, the optimized structural parameters are enumerated in Table 1. For the ZB $Mg_{0.75}$ $Ti_{0.25}Y$ (Y = S, Se, Te) crystal structures, we have premeditated the difference in energy ($\Delta E = E_{NM} - E_{FM}$) between FM and NM states by optimization of the crystal structure. The plots of optimization are displayed in Fig. 1, and energy difference values are given in Table 1 which implies that FM states of $Mg_{0.75}Ti_{0.25}S$, $Mg_{0.75}Ti_{0.25}Se$, and $Mg_{0.75}Ti_{0.25}Te$ are of lower energies than that of their NM states. Consequently, the compounds being studied are stable in FM state. To confirm the thermodynamic permanence in FM state, with ZB crystal structures, we also premeditated the enthalpy of formation ($\Delta H$) from the following relation:

$$\Delta H = E_{\text{Total}}\left(\text{Ti}_l\text{Mg}_m\text{S}_n/\text{Se}n/\text{Te}_n\right) - lE_{\text{Ti}} - mE_{\text{Mg}} - nE_{\text{S/Se/Te}} \quad (1)$$

where the energies $E_{\text{Total}}\left(\text{Ti}_l\text{Mg}_m\text{Sn/Se}_n/\text{Te}_n\right)$, $E_{\text{Ti}}$, $E_{\text{Mg}}$, and $E_{\text{S/Se/Te}}$ are related to the lowest total ground state energy of $Mg_mTi_lY_n$ ($Y_n$ = $S_n$, $Se_n$, and $Te_n$) alloys and the individual ground state energies per atom of Ti, Mg, S, Se, and Te correspondingly, where $l, m, n$ show contribution from Ti, Be, and S/Se/Te atoms for the unit cell formation. The enthalpy of formation gives the negative values as given in Table 1, which makes sure that ZB $Mg_{0.75}Ti_{0.25}Y$ (Y = S, Se, Te) have high stability and their evolution in FM phase are moderately conceivable.

From the structural optimization (Fig. 1), the equilibrium lattice constant ($a_0$) and bulk modulus ($B_0$) were derived for binary semiconductors and their ternary $Mg_{0.75}Ti_{0.25}S$, $Mg_{0.75}Ti_{0.25}Se$, and $Mg_{0.75}Ti_{0.25}Te$ alloys (see data in Table 1). The analysis of data shows that the lattice constant of ternary $Mg_{0.75}Ti_{0.25}S$, $Mg_{0.75}Ti_{0.25}Se$, and $Mg_{0.75}Ti_{0.25}Te$ alloys increases and bulk modulus decreases as compared to binary alloys MgS, MgSe, and MgTe. However, the lattice constant ($a_0$) increases from $Mg_{0.75}Ti_{0.25}S$, $Mg_{0.75}Ti_{0.25}Se$, to $Mg_{0.75}Ti_{0.25}Te$ because ionic radius down the group (S to Te) increases due to addition of shells. The value of $\Delta E$ also increases from S to Te that shows that the ternary alloys $Mg_{0.75}Ti_{0.25}S$, $Mg_{0.75}Ti_{0.25}Se$, and $Mg_{0.75}Ti_{0.25}Te$ have different values of ferromagnetism with different Curie temperatures [30–33].

### 3.2 Mechanical Properties

To elaborate the mechanical and dynamical behavior of crystals, the knowledge of elastic constants is highly meaningful. Moreover, elastic constants describe materials behavior before and after applied stress [34]. We have performed ab initio calculations to compute elastic moduli $C_{ij}$ by calculating stress tensor components for small strain. These constants perform a magnificent part in revealing substantial information regarding the steadiness and stiffness of materials. The method used to evaluate these constants was developed by Chapin and implemented in Wien2k code [35] which already has been applied in some prior studies [36–38] with successful results. Since the investigated materials have cubic symmetry, it is necessary to calculate merely three independent elastic parameters $C_{11}$, $C_{12}$, and $C_{44}$ for complete description of their mechanical properties. Hence,

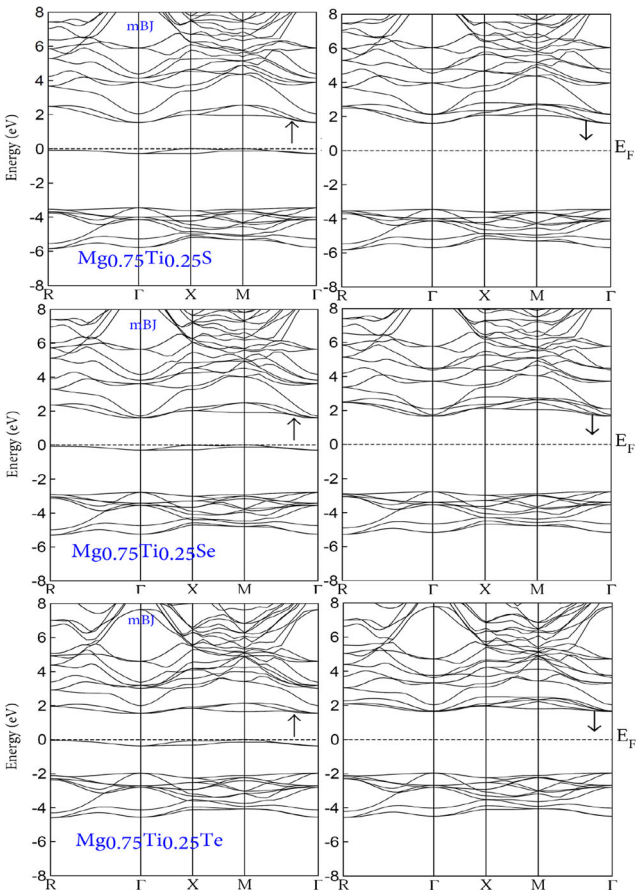


**Fig. 2** Spin polarized band structures of $Mg_{0.75}Ti_{0.25}Y$ (Y = S, Se, Te) alloys in majority spin-up (*upwards arrow*) and minority spin-down (*downwards arrow*) states using mBJGGA functional

three equations are needed to perceive these constants [39]. The generalized Hooke's law provide a connection between stresses ($s$) and strains ($\varepsilon$) to obtain elastic moduli as follows: The Born stability criteria was used to [40] defines mechanical stability of a cubic crystal. The bulk modulus estimated by using the relation $B = (1/3)(C_{11} + 2C_{12})$, as well as by energy minimization, has nearly the equal values (see Table 2). This is the reliability of the determined results for the studied compounds. Kleinman parameter ($\zeta$) speaks about dominate character of either bond bending or bond stretching in cubic materials. Its value drops to 0 and 1 for minimizing bond bending and stretching, respectively. In the present study, bond stretching is dominating over bond bending [41].

In engineering sciences, the knowledge of elastic anisotropy is of great importance as it states that how microcracks are possible to be infiltrated in materials [42]. In this context, we have evaluated the anisotropy factor A using obtained elastic constants and it stands 1 for an isotropic material while any deviation (lower or higher) from 1 indicates anisotropy [43]. The degree of anisotropy is measured as magnitude of the deviation from 1. Referring to Table 2, the studied compounds are anisotropic materials as A undergoes deviation from unity. For the sake of evaluation of

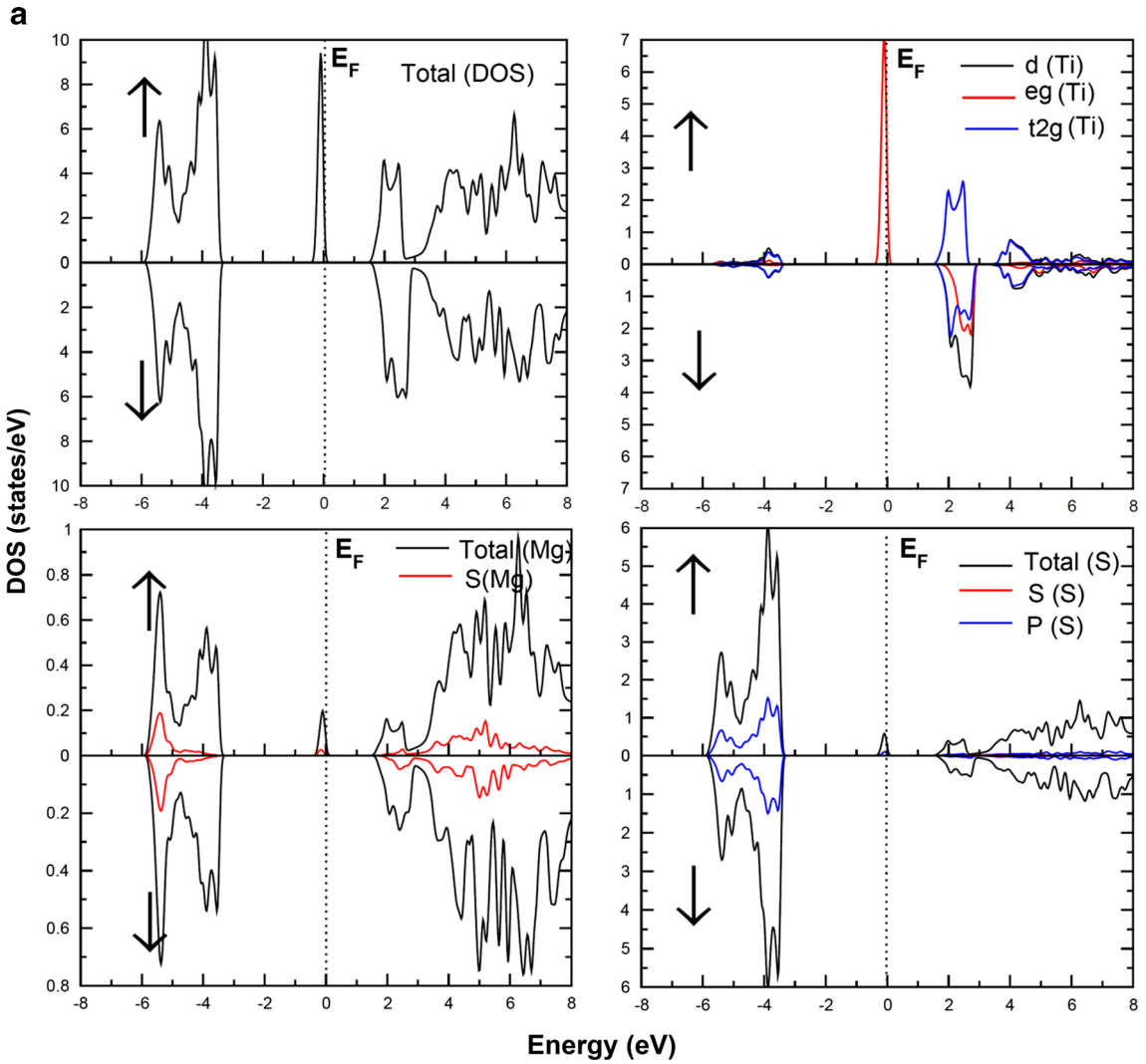


**Fig. 3** **a** The calculated total density of states (TDOS) along DOS with partial Ti, Mg, and S sites for $Mg_{0.75}Ti_{0.25}S$ alloy for majority spin-up (*upwards arrow*) and minority spin-down (*downwards arrow*) configuration using mBJGGA functional. **b** The calculated total density of states (TDOS) along DOS with partial Ti, Mg, and Se sites for $Mg_{0.75}Ti_{0.25}Se$ alloy for majority spin-up (*upwards arrow*) and minority spin-down (*downwards arrow*) configuration using mBJGGA functional. **c** The calculated total density of states (TDOS) along DOS with partial Ti, Mg and Te sites for $Mg_{0.75}Ti_{0.25}Te$ alloy for majority spin-up (*upwards arrow*) and minority spin-down (*downwards arrow*) configuration using mBJGGA functional

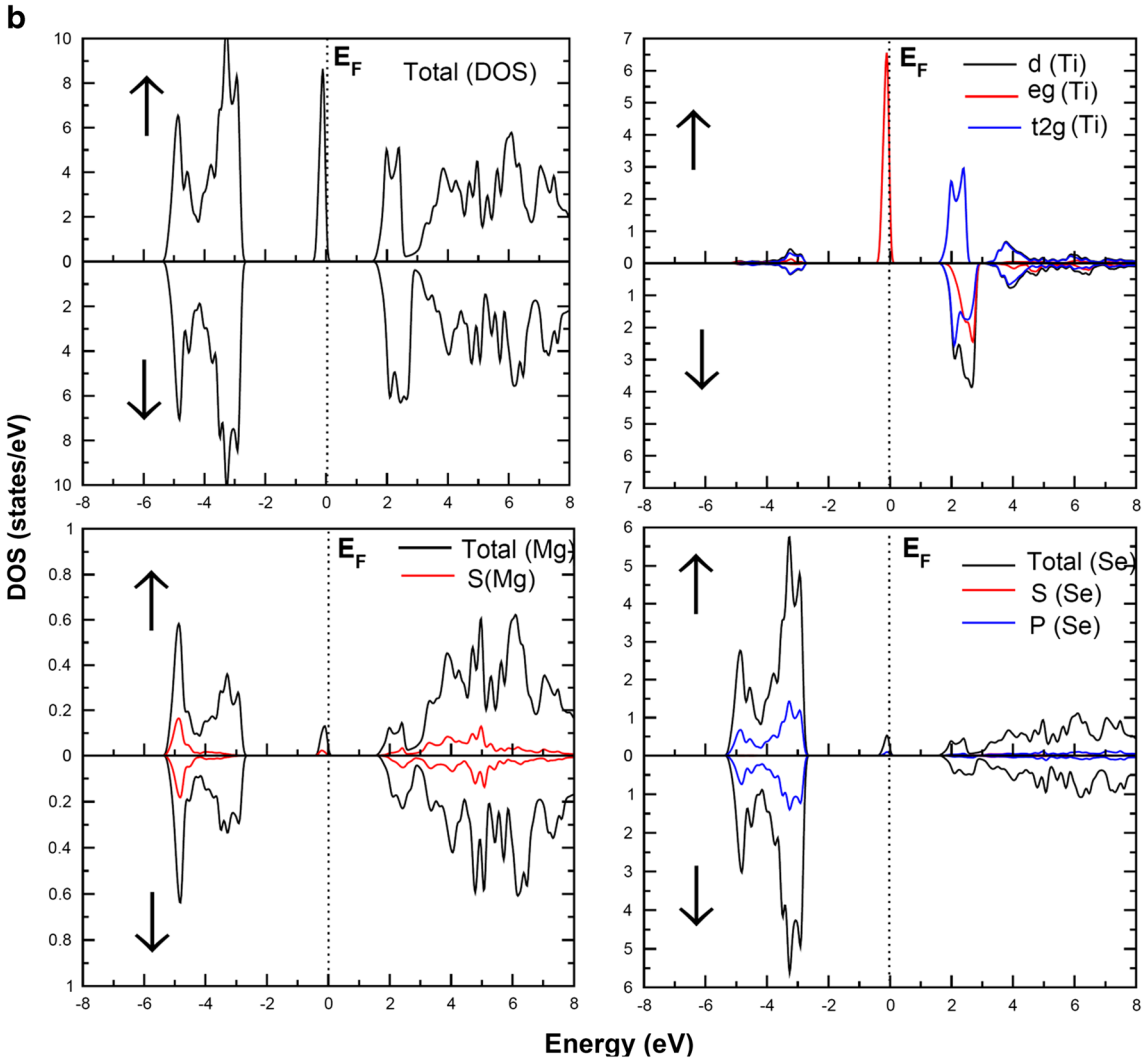


**Fig. 3** (continued)

moduli for the proposed materials, the Voigt-Reuss-Hill [44] approximation has been employed because our materials are generally polycrystalline. According to this approximation, the approximated modulus can be driven from the average of the two recognized bounds for mono-crystals as suggested by Voigt [45] and Reuss [46]. In this regard, the abovementioned moduli for cubic structures are worked out from the relations given in Ref. [47]. Moreover, Young's modulus ($E$) and the Poisson's ratio ($\nu$) have also been premeditated. Both of these factors are linked with bulk modulus ($B$), and Shear modulus ($G$) by the equations given in Ref. [48, 49]. The estimated elastic moduli for the binary MgY and its alloys $Mg_{0.75}Ti_{0.25}S$, $Mg_{0.75}Ti_{0.25}Se$, and $Mg_{0.75}Ti_{0.25}Te$ are listed in Table 2. Higher value of E places a material in the category of stiffer materials. Since the value of E decreases while going from S to Te, the alloy $Mg_{0.75}Ti_{0.25}S$ is stiffer than that of $Mg_{0.75}Ti_{0.25}Se$ and $Mg_{0.75}Ti_{0.25}Te$. Among the determined elastic parameters, Poisson's ratio is more capable of explaining bonding forces operational in a material. The upper and lower limits defined for $\nu$ are 0.5 and 0.25, respectively [50]. Since the value of $\nu$ is laying within 0.25–0.5 for all under observation alloys, so the central inter-atom forces are set in these alloys. The covalent and ionic materials can also be distinguished with Poisson's ratio value which is typically 0.1 and 0.25 for covalent and ionic materials, respectively. On the basis of estimated values of $\nu$, all alloys are ionic. Furthermore, the critical value 0.26 of Poisson's ratio separates a brittle material from a ductile one [51]. It is obvious from our $\nu$ values that all the proposed materials are ductile. The brittle and ductile nature of a compound can also be characterized by Pugh's ratio (B/G) whose critical value is 1.75. Referring to Table 2, B/G value is 2.47 for $Mg_{0.75}Ti_{0.25}S$, 2.29 for $Mg_{0.75}Ti_{0.25}Se$, and 1.79 for $Mg_{0.75}Ti_{0.25}Te$ classifying these compounds as ductile. So, ductile nature makes them suitable candidate for device fabrication.

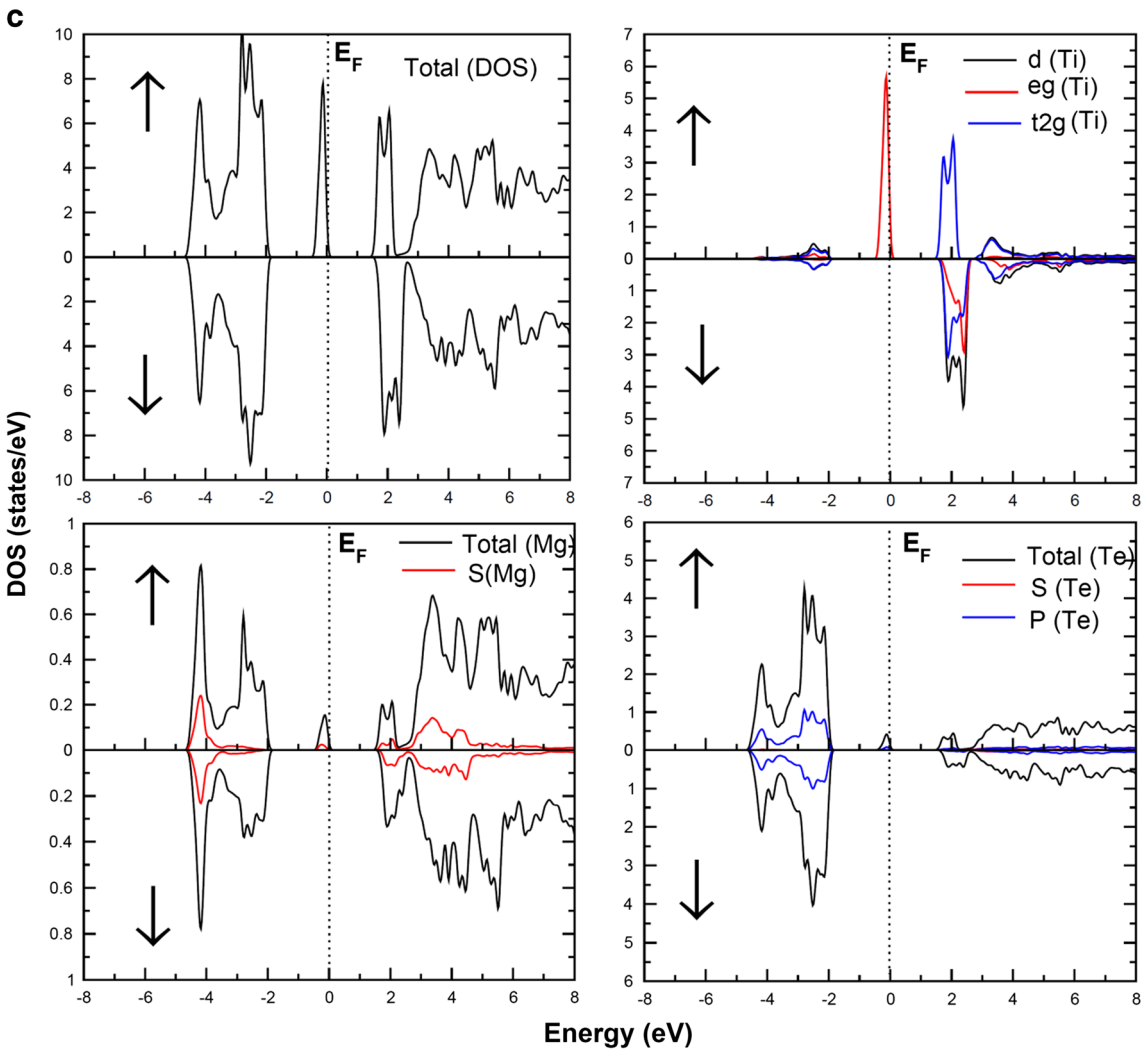


**Fig. 3** (continued)

### 3.3 Electronic Properties

The electronic band structures and density of states (DOS) are embraced in the electronic properties of $Ti_{0.25}Mg_{0.75}S$, $Ti_{0.25}Mg_{0.75}Se$, and $Ti_{0.25}Mg_{0.75}Te$ compounds for spin-up and spin-down arrangements along the high symmetry directions in the first Brillouin zone have been calculated by using mBJLDA functional. In this study, the calculated equilibrium lattice constants were used to run the self-consistent calculations. It is clear from Fig. 2 that the band gap is symmetric in spin-down channel across the $E_F$ because of splitting of Ti atom 3*d* degenerate states without losing the semiconducting character of MgS, MgSe, and MgTe, while the spin-up channel shows the metallic character. Therefore, the overall contributions of both spin-up and spin-down channel show the half-metallic character in these compounds. Furthermore, it is clear that in the spin-down channel, less number of electrons exist as likened to that in spin-up channel. A valuable explanation about total (TDOS) and partial density of states (PDOS) delivers profound apprehend of band structures of $Ti_{0.25}Mg_{0.75}S$, $Ti_{0.25}Mg_{0.75}Se$, and $Ti_{0.25}Mg_{0.75}Te$, as depicted in Fig. 3a–c. The density of states (DOS) plot clearly shows that 3*d*-state of Ti splits across the $E_F$ within $E_g$ of host semiconductors and retains a band gap in down spin channel. Therefore, the doping of Ti impurity does not disturb the semiconducting property of MgS, MgSe, and MgTe in the spin-down channel. This behavior of $Ti_{0.25}Mg_{0.75}S$, $Ti_{0.25}Mg_{0.75}Se$, and $Ti_{0.25}Mg_{0.75}Te$ compounds depicts the half-metallic character. Moreover, the low energy region from −5 to −3 eV for $Ti_{0.25}Mg_{0.75}S$, −5 to −2.5 eV for $Ti_{0.25}Mg_{0.75}Se$, and −5 to −2 eV for $Ti_{0.25}Mg_{0.75}Te$ compounds shows the weak interaction of p-state and s-state of S/Se/Te with 3d-state of Ti, while across the Fermi level (from energy region −1 to 6 eV), the interaction of *p*-state of anion with 3*d*-state of Ti impurity exhibit strong $p - d$

**Table 3** Energy splitting $\Delta_x(d)$, conduction band edge splitting ($\Delta E_C$) and valance band edge splitting ($\Delta E_V$) and exchange constants ($N\alpha$ and $N\beta$) calculated for all three $Mg_{0.75}Ti_{0.25}S$, $Mg_{0.75}Ti_{0.25}Se$ and $Mg_{0.75}Ti_{0.25}Te$ DMS alloys

| Compound | $\Delta_x(d)$ | $E_{crystal}$ | $\Delta E_C$ (eV) | $\Delta E_V$ (eV) | $N\alpha$ | $N\beta$ |
|---|---|---|---|---|---|---|
| $Mg_{0.75}Ti_{0.25}S$ | 2.71 | 2.13 | 0.04 | −3.40 | 0.214 | −18.18 |
| $Mg_{0.75}Ti_{0.25}Se$ | 2.69 | 2.07 | 0.07 | −2.72 | 0.368 | −14.28 |
| $Mg_{0.75}Ti_{0.25}Te$ | 2.08 | 1.89 | 0.17 | −1.90 | 0.873 | −s10.16 |

hybridization. The cause of this hybridization being week in the low energy region is due to the tendency of Ti $d$-states of being localized. There is a creation of extensive energy band gap in spin-down channel across the Fermi level.

From Fig. 3a, b and c the $p$ states of S, Se and Te respectively, and the $d$ states of Ti show hybridization, which leads to the bandgap in the spin down channel. As well as unraveling the symmetry of two- and threefold perverted states ($e_g$ and $t_{2g}$), the $p-d$ hybridization performs a significant part in the creation of FM in the studied materials by producing the dual exchange interaction. The states $e_g$ and $t_{2g}$ appear owing to drive of fivefold perverted 3$d$-states of Ti, and the central cause of state splitting is the tetrahedral atmosphere created by S/Se/Te atoms. Furthermore, in the spin-up case, the $e_g$ states exist in the energy zone $E_F$ <0, whereas the $t_{2g}$ states are enclosed in the situated of $E_F$ in VB and CB as shown in Fig. 3a–c. Conversely in spin-down, both of the symmetry states are completely situated in CB ($E_F$ >0). Moreover, the difference of spin-up and spin-down peaks of Ti-3$d$corresponds to the spin exchange splitting energy ($\Delta_x(d)$). The values of spin interchange splitting energies between the spin-up and spin-down Ti 3$d$-states and crystal field energies for $Ti_{0.25}Mg_{0.75}S$, $Ti_{0.25}Mg_{0.75}Se$, and $Ti_{0.25}Mg_{0.75}Te$ alloys are presented in Table 3. The greater values of exchange splitting energies than crystal field energies lower the energy of the system because strong $p-d$ hybridization favors the ferromagnetism in $Ti_{0.25}Mg_{0.75}S$, $Ti_{0.25}Mg_{0.75}Se$, and $Ti_{0.25}Mg_{0.75}Te$ alloys [18].

### 3.4 Electron Charge Density

The charge density for $Ti_{0.25}Mg_{0.75}S$, $Ti_{0.25}Mg_{0.75}Se$, and $Ti_{0.25}Mg_{0.75}Te$ alloys was also examined (by implementing mBJLDA approximation) by taking into account the spin-up and spin-down configuration in (110) crystallographic plane. Figure 4 shows the spin-polarized contour plots of $Ti_{0.25}Mg_{0.75}S$, $Ti_{0.25}Mg_{0.75}Se$, and $Ti_{0.25}Mg_{0.75}Te$ alloys for spin-up (↑) and spin-down (↓) configuration. The contour plot (Fig. 4) shows the partially ionic and partially covalent nature of bonds between Ti-S, Ti-Se, and Ti-Te atoms. The charge transfer was observed between cations and anions which reflected the electronegativity difference among Mg, Te, and Ti. Thus, stronger ionic bond was found in Ti-S/Ti-Se/Ti-Te than Mg-S/Mg-Se/Mg-Te due to greater electronegativity difference in Mg-S/Se/Te as compared to Ti-S/ Ti-Se/ Ti-Te atoms. Comparing the contour plots of all three DMS, more charge transfer was observed in $Ti_{0.25}Mg_{0.75}S$ and $Ti_{0.25}Mg_{0.75}Se$ than $Ti_{0.25}Mg_{0.75}Te$ alloys. Further, it can also be seen that the $d$-states of magnetic ion has strong contribution in bonding for spin-up (↑) state, thus leading to major part of spin charge density. While $d$-states of magnetic ion has less contribution in bonding for spin-down (↓) state, thus disturbing the spherically symmetric charge distribution. On the other hand, Ti-S, Ti-Se, and Ti-Te bonds have a higher ionic character due to the higher electronegativity difference. The charge residing around Mg atom is contributed from $s$ states; however, both $s$ and $p$ states are responsible gather charge around anions.

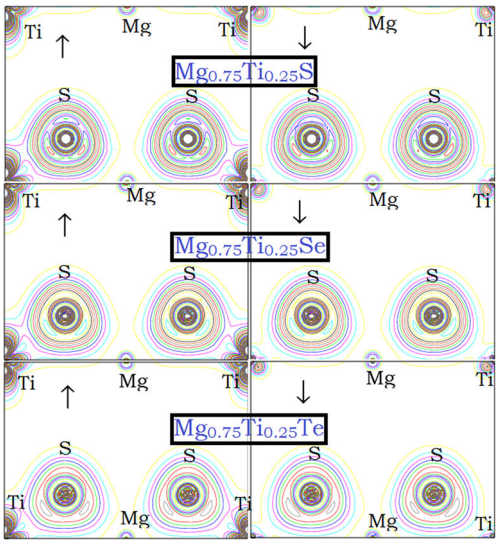


**Fig. 4** Electron density plots of $Mg_{0.75}Ti_{0.25}Y$ (Y = S, Se, Te) alloys for both spin-up (*upwards arrow*) and spin-down (*downwards arrow*) configurations using mBJGGA functional

**Table 4** Calculated magnetic moment at Mg, Ti and Y (Y = S, Se, Te) sites in $Mg_{0.75}Ti_{0.25}Y$ alloys

| Compound | Magnetic moments (in terms of Bohr magnetron, $\mu_B$) | | | |
|---|---|---|---|---|
| | Total ($\mu_B$) | Mg-site ($\mu_B$) | Y-site ($\mu_B$) | Ti-site ($\mu_B$) |
| $Mg_{0.75}Ti_{0.25}S$ | 2.000 | 0.02051 | −0.00185 | 1.49579 |
| $Mg_{0.75}Ti_{0.25}Se$ | 2.000 | 0.01439 | −0.00596 | 1.52332 |
| $Mg_{0.75}Ti_{0.25}Te$ | 2.000 | 0.01900 | −0.01190 | 1.55856 |

### 3.5 Magnetic Behavior

To evaluate the magnetic properties of $Ti_{0.25}Mg_{0.75}S$, $Ti_{0.25}Mg_{0.75}Se$, and $Ti_{0.25}Mg_{0.75}Te$ alloys, the total and local magnetic moments are calculated with mBJLDA and are listed in Table 4. Although, the calculated values of magnetic moment vary by employing different exchange correlation functional, it is noticeable that total magnetic moment values are identical for all the investigated compounds and main contribution comes from local magnetic moment of Ti ion. The electrons spin density (shown in Fig. 5) explains the overall atomic contribution to magnetic moment (taking the net contribution of electrons spin-up and spin-down state magnetic moments). The yellow flowers around the Ti atoms show its major contribution to magnetic moment as illustrated earlier in Table 3.

For the sake of studying the role of conduction and valence bands in exchange splitting process, the knowledge of exchange constants ($N_0\alpha$ and $N_0\beta$) is necessary. The realization of these bands' role is appropriate to parameterize conduction and valence bands spin splitting. This explanation is consistent with Hamiltonian-based mean field theory by the following equation [52, 53]:

$$H = -N_0\beta s.S \tag{2}$$

where $N_0$ is cation concentration, $\beta$ denotes the *pd* exchange integral, $s$ and $S$ represent hole spin and Ti spin, respectively. Similarly, the conduction band spin-splitting can be calculated on the basis of same Hamiltonian with exchange constant $N_0\alpha$. So, the edge splitting of conduction band ($\Delta E_C = E_C^{\downarrow} - E_C^{\uparrow}$) and valence band ($\Delta E_V = E_V^{\downarrow} - E_V^{\uparrow}$) are serving to estimate both of the exchange constants using the following equations:

$$N_O\alpha = \frac{\Delta E_C}{x\langle S\rangle} \text{ and } N_O\beta = \frac{\Delta E_V}{x\langle S\rangle} \tag{3}$$

Table 3 shows the obtained values of $\Delta E_c$, $\Delta E_v$, $N_0\alpha$, and $N_0\beta$. The exchange splitting energy $\Delta_x(pd)$ which is the difference between maxima's of valence bands for spin-down and spin-up (i.e., $\Delta_x(pd) = E_V^{\downarrow} - E_V^{\uparrow}$), respectively. This energy is commonly used to compute magnetic properties of magnetic semiconductors [9, 29]. From Table 3, it is evident that the exchange splitting energy $\Delta_x(pd)$ decreases while going from S to Te which is explained by the increasing differences in the electronegativity values and the increasing covalent bonding nature discussed earlier. The effective potential is more attractive for spin-down than that of spin-up as evident from the negative values of $\Delta_x(pd)$, and it is in accordance with previous studies of the Ti-doped systems [54]. These findings confirm that *pd* coupling in the conduction band of $Ti_{0.25}Mg_{0.75}S$, $Ti_{0.25}Mg_{0.75}Se$, and

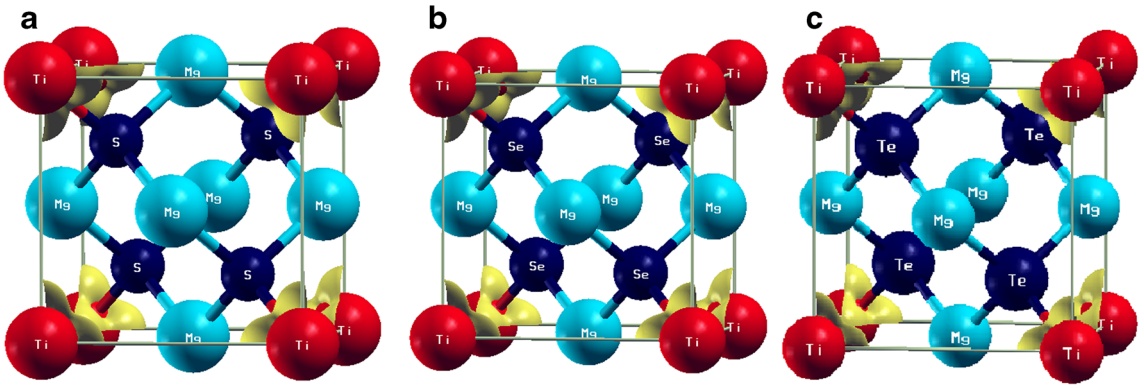


**Fig. 5** Plots of spin density for (**a**) $Mg_{0.75}Ti_{0.25}S$, (**b**) $Mg_{0.75}Ti_{0.25}Se$, and (**c**) $Mg_{0.75}Ti_{0.25}Te$ alloys, where *yellow flowers* represent magnetic moment contribution of each atom

$Ti_{0.25}Mg_{0.75}Te$ alloys, due to Ti impurity, is ferromagnetic in nature.

## 4 Conclusion

In conclusion, the structural, mechanical, electronic, and magnetic behavior of $Ti_{0.25}Mg_{0.75}S$, $Ti_{0.25}Mg_{0.75}Se$, and $Ti_{0.25}Mg_{0.75}Te$ DMS system have been investigated by means of first-principles DFT calculations based on the FP-LAPW + lo method. On the basis of our results, following main conclusions are drawn:

(i) The equilibrium lattice constant of MgY compounds increase with the addition of Ti-dopant.
(ii) T he $Ti_{0.25}Mg_{0.75}S$, $Ti_{0.25}Mg_{0.75}Se$, and $Ti_{0.25}Mg_{0.75}Te$ alloys are found to be in ferromagnetic (FM) phase. The negative enthalpies of formation for all three alloys confirm the stability of FM phase.
(iii) The $Ti_{0.25}Mg_{0.75}S$, $Ti_{0.25}Mg_{0.75}Se$, and $Ti_{0.25}Mg_{0.75}Te$ alloys exhibit strong ductile behavior.
(iv) The density of states and band structures $Ti_{0.25}Mg_{0.75}S$, $Ti_{0.25}Mg_{0.75}Se$, and $Ti_{0.25}Mg_{0.75}Te$ alloys exhibit half-metallic ferromagnetic behavior.
(v) For all three alloys, large magnetic moment is observed at the magnetic atomic sites, while small magnetic moments also appear at the non-magnetic sites (Mg and S/Se/Te) caused by the hybridization of $p$- and $d$-states.

**Acknowledgment** The author (Asif Mahmood) would like to extend his sincere appreciations to the Deanship of Scientific Research at King Saud University for funding this Prolific Research Group (PRG-1436-26).

## References

1. Shirai, M.: J. Appl. Phys. **93**, 6844 (2003)
2. Wong, K.M., Alay-e-Abbas, S.M., Shaukat, A., Fang, Y., Lei, Y.: J. Appl. Phys. **113**, 014304 (2013)
3. Amin, B., Arif, S., Ahmad, I., Maqbool, M., Ahmad, R., Goumri-Said, S., Prisbrey, K.: J. Electronic Materials **40**, 1428 (2011)
4. Sajjad, M., Zhang, H.X., Noor, N.A., Alay-e-Abbas, S.M., Younas, M., Abid, M., Shaukat, A.: J. Supercond. Nov. Magn. **27**, 2327 (2014)
5. Noor, N.A., Ikram, N., Ali, S., Nazir, S., Alay-e-Abbas, S.M., Shaukat, A.: J. Alloys compd. **507**, 356 (2010)
6. Noor, N.A., Tahir, W., Aslam, F., Shaukat, A.: Physica B **407**, 943 (2012)
7. Noor, N.A., Ali, S., Shaukat, A.: J. Phys. Chem. Solids **72**, 836 (2011)
8. Kılıç, A., Kervan, N., Kervan, A.: J. Supercond. Nov. Magn **28**, 1767 (2015)
9. Furdyna, J.K.: J. Appl. Phys. **64**, R29 (1988)
10. Boutaleb, M., Doumi, B., Sayede, A., Tadjer, A., Mokaddem, A.: J. Supercond. Nov. Magn **28**, 143 (2015)
11. Dwarakanadha Reddy, Y., Reddy, B.K., Sreekantha Reddy, D., Reddy, D.R.: J. Spectrochim. Acta Part A **70**, 934 (2008)
12. Feng, Q.J., Shen, D.Z., Zhang, J.Y., Li, B.H., Zhang, Z.Z., Lu, Y.M., Fan, X.W.: Mater. Chem. Phys. **112**, 1106 (2008)
13. Pearton, S.J., Abernathy, C.R., Norton, D.P., Hebard, A.F., Park, Y.D., Boatner, L.A., Budai, J.D.: Mater. Sci. Engin. R **40**, 137 (2003)
14. Zaari, H., Boujnah, M., El hachimi, A.G., Benyoussef, A., El Kenz, A.: Comp. Mater. Sci. **93**, 91–96 (2014)
15. Dahmane, F., Tadjer, A., Doumi, B., Mesri, D., Aourag, H.: J. Supercond. Nov. Magn **26**, 3339 (2013)
16. Mahmood, Q., Javed, A., Murtaza, G., Alay-e-Abbas, S.M.: Mater. Chem. Phys. **162**, 831 (2015)
17. El Amine Monir, M., Baltache, H., Murtaza, G., Khenata, R., Bin Omra, S., Uğur, S., Benalia, S., Rached, D.: Inter. J. Modern Phys. B **28**, 1450080 (2014)
18. Drief, F., Tadjer, A., Mesri, D., Aourag, H.: Catal. Today **89**, 343–355 (2004)
19. Varshney, D., Kaurav, N., Sharma, U., Singh, R.K.: J. Phys. Chem. Solids **69**, 60 (2008)
20. Zaari, H., Boujnah, M., El Hachimi, A., Benyoussef, A., El Kenz, A.: Opt. Quant Electron **46**, 75 (2014)
21. Rabaha, M., Abbar, B., Al-Douri, Y., Bouhafs, B., Sahraoui, B.: Mater. Sci. Engin B **100**, 163 (2003)
22. Blaha, P., Schwarz, K., Madsen, G.K.H., Kvasnicka, D., Luitz, J.: An Augmented-Plane-Wave + Local Orbitals Program for Calculating Crystal properties, Karlheinz Schwarz, Techn. Wien, Austria (2001)
23. Hohenberg, P., Kohn, W.: Phys. Rev. **136**, B864 (1964)
24. Wu, Z., Cohen, R.E.: Phys. Rev. **B73**, 235116 (2006)
25. Becke, A.D., Johnson, E.R.: J. Chem. Phys **124**, 221101 (2006)
26. Singh, D.J.: Phys. Rev. B **82**, 205102 (2010)
27. Guo, S.-D., Liu, B.-G.: Euro Phys. Lett. **93**, 47006 (2011)
28. Arda, L., Ackgoz, M., Gungor, A.: J. Supercond. Nov. Magn. **25**, 2701 (2012)
29. Alay-e-Abbas, S.M., Wong, K.M., Noor, N.A., Shaukat, A., Lei, Y.: Solid State Sci. **14**, 1525 (2012)
30. Amari, S., M eçabih, S., Abbar, B., Bouhafs, B.: Comp. Mater. Sci. **50**, 2785 (2011)
31. Soundararajan, D., Mangalaraj, D., Nataraj, D., Dorosinskii, L., Kim, K.H.: Mater. Lett. **87**, 113 (2012)
32. Guo, M., Gao, G., Hu, Y.: J. Magn. Magn. Mater. **323**, 122 (2011)
33. Amari, S., M eçabih, S., Abbar, B., Bouhafs, B.: J. Magn. Magn. Mater. **324**, 2800 (2012)
34. Reshak, H., Jamal, M.: J. Alloys Compd. **543**, 147 (2012)
35. Blaha, P., Schwarz, K., Medsen, G.K.H., Kvasnicka, D., Luitz, J., Schwartz, K.: Techn. Universitad, Wien Austria (2001)
36. Haj Hassan, F.El.., Akbarzadeh, H.: Comput. Mater. Sci. **38**, 362 (2006)
37. Khenata, R., Bouhemadou, A., Sahnoun, M., Reshak A.H., Baltache, H., Rabah, M.: Comput. Mater. Sci. **38**, 29 (2006)
38. Bouhemadou, A., Khenata, R., Kharoubi, M., Seddik, T., Reshak, A.H., Al-Douri, Y.: Comput. Mater. Sci. **45**, 474 (2009)
39. El Amine Monir, M., Baltache, H., Khenata, R., Murtaza, G., Azam, S., Bouhemadou, A., Al-Douri, Y., BinOmran, R.A.: J. Magn. Magn. Mater **378**, 41 (2015)
40. Nye, F.: Physical properties of crystals: Their representation by tensors and matrices. Oxford University Press, Oxford (1985)
41. Jamal, M., Jalali Asad abadi, S., Ahmad, I., Rahnamaye Aliabad, H.A.: Comput. Mater. Sci. **95**, 592 (2014)

42. Tvergaard, V., Hutshinson, J.W.: J. Am. Ceram. Soc. **71**, 57 (1988)
43. Hayatullah, Murtaza, G., Khenata, R., Mohammad, S., Naeem, S., Khalid, M.N., Manzar, A.: Physica B **420**, 15 (2013)
44. Hill, R.: Proc. Phys. Soc. London **A65**, 349 (1952)
45. Voigt, W.: Lehrbush Der Kristallphysik. Taubner, Leipzig (1928)
46. Reuss, A., Angew, A.: Mat. Phys. **9**, 49 (1929)
47. Wu, Z.J., Zhao, Xiang, H.P., Hao, X.F., Liu X.J.: J. Meng. Phys. Rev. B **76**, 054115 (2007)
48. Peng, F., Chen, D., Fu, H., Cheng, X.: Phys. Status Solidi B **246**, 71 (2009)
49. Fu, H., Li, D., Peng, F., Gao, T., Cheng, X.: Comput. Mater. Sci. **44**, 774 (2008)
50. Haddou, A., Khachai, H., Khenata, R., Litimein, F., Bouhemadou, A., Murtaza, G., Alahmed, Z.A., Bin- Omran, S., Abbar, B.: J. Mater. Sci. **48**, 8235 (2013)
51. Pugh, S.F.: Philos. Mag. **45**, 823 (1953)
52. Gaj, G.A., Planel, R., Fishman, G.: Solid State Commun. **29**, 435 (1979)
53. Sanvito, S., Ordejon, P., Hill, N.A.: Phys. Rev. B **63**, 165206 (2001)
54. Mahmood, Q., Alay-e-Abbas, S.M., Mahmood, A., Yaseen, M., Mahmood, I., Noor, N.A.: J Supercond. Nov. Magn. **29**, 521 (2016)
55. Wyckoff, R.W.G.: Crystal Structures. Wiley, New York (1963)
56. Waag, A., Heinke, H., Scholl, S., Becker, C.R., Landwehr, G.: J. Cryst. Growth **131**, 607 (1993)
57. Drief, F., Tadjer, A., Mesri, D., Aourag, H.: Catalysis Today **89**, 343 (2004)
58. Cardona, M., Harbeke, G.: Phys. Rev. A **137**, 1467 (1965)
59. Okuyama, H., Nakano, K., Miyajima, T., Akimoto, K.: J. Crystal Growth **117**, 139 (1992)
60. Parker, S.G., Reinberg, A.R., Pinnell, J.E., Holton, W.C.: J. Electrochem. Soc. **118**, 979 (1971)